LBL-32523
UC-404
Preprint

Lawrence Berkeley Laboratory
UNIVERSITY OF CALIFORNIA

CHEMICAL SCIENCES DIVISION

Submitted to Physical Review B

Zero-Field Splitting of Cm^{3+} in $LuPO_4$ Single Crystals

W.K. Kot, N.M. Edelstein, M.M. Abraham, and L.A. Boatner

May 1993

Prepared for the U.S. Department of Energy under Contract Number DE-AC03-76SF00098

DISCLAIMER

LBL-32523

ZERO-FIELD SPLITTING OF Cm^{3+} IN $LuPO_4$ SINGLE CRYSTALS

W. K. Kot and N. M. Edelstein
Chemical Sciences Division
Lawrence Berkeley Laboratory, University of California
Berkeley, California 94720

and

M. M. Abraham and L. A. Boatner
Solid State Division, Oak Ridge National Laboratory
Oak Ridge, TN 37831-6056

This research was sponsored by the Division of Materials Sciences, U.S. Department of Energy under Contract No. DE-AC05-84OR21400 with Martin Marietta Energy Systems, Inc., and by the Director, Office of Energy Research, Office of Basic Energy Sciences, Chemical Sciences Division of the U.S. Department of Energy under Contract No. DE-AC03-76SF00098.

ZERO-FIELD SPLITTING OF Cm^{3+} IN $LuPO_4$ SINGLE CRYSTALS

W. K. Kot and N. M. Edelstein
Chemical Sciences Division
Lawrence Berkeley Laboratory, University of California
Berkeley, California 94720

and

M. M. Abraham and L. A. Boatner
Solid State Division, Oak Ridge National Laboratory
Oak Ridge, TN 37831-6056

Abstract

Electron paramagnetic resonance (EPR) spectroscopy has previously been employed in investigating excited levels of the ground-state manifold of the $5f^7$-configuration-ion Cm^{3+} diluted in single crystals of the tetragonal-symmetry, zircon-structure hosts $LuPO_4$ and YPO_4. The three intra-doublet resonances that were observed in these earlier studies, however, were significantly broadened due to radiation damage arising from the use of the 18.1 y half-life isotope ^{244}Cm. In the present work, the isotope ^{248}Cm ($T_{1/2} = 3.4 \times 10^5$ y) with a significantly lower specific activity has been incorporated in $LuPO_4$ host single crystals in order to reduce the internal radiation-induced damage that can broaden both EPR and optical transitions. By employing these ^{248}Cm-doped $LuPO_4$ samples, it has been possible to observe an additional "inter-doublet" transition for Cm^{3+}, to perform more accurate measurements of the various "intra-doublet" transitions at higher microwave frequencies, and to obtain new optical absorption and fluorescence data for this system. These new EPR and optical results have led to a more complete and accurate determination of the energy-level structure of Cm^{3+}. Additionally, it has been possible to detect magnetic resonance transitions for the Cm^{3+} ion at room temperature for the first time.

INTRODUCTION

Due to the essentially spherical symmetry of the wave function associated with the predominantly L = 0 ground states of transition-series ions with half- filled shells (so-called S-state ions), only higher-order interactions are possible with a surrounding crystalline environment. Such higher-order interactions do, in fact, occur and result in splittings of S ground states that are observed experimentally. In the course of the past almost 60 years, various mechanisms or combinations of mechanisms have been proposed to account for the ground-state splittings of S-state ions as revealed in the relatively extensive experimental EPR and magnetic susceptibility results for ions of this type.

Despite the various prior theoretical attempts to account for the experimental findings, the nature of the interactions responsible for the ground-state splittings of S-state ions is, in general, still not well understood. In the particular case of S-state ions associated with half-filled shells in the 4f and 5f transition series (i.e., $4f^7$- and $5f^7$- electronic configuration ions such as Eu^{2+}, Gd^{3+}, and Tb^{4+} or Am^{2+}, Cm^{3+} and Bk^{4+}), however, the significant differences that are found in the magnitude of the experimentally determined ground-state splittings can be qualitatively accounted for by a consideration of the effects of intermediate-coupling. For example, in the lanthanide series the $4f^7$-configuration Gd^{3+} ion has a ground-state wave function that is 98% $^8S_{7/2}$. For the $5f^7$-configuration ion Cm^{3+}, which has a free-ion spin-orbit coupling parameter that is approximately twice that of Gd^{3+}, increased intermediate-coupling effects lead to a larger admixture of other states (still having J = 7/2 but with different values of L and S) into the $^8S_{7/2}$ ground state. This significantly larger admixture of non L =0 states results in a Cm^{3+} ground-state wavefunction that is only 79% pure $^8S_{7/2}$. These significant differences in the non-S-state character of the ground-state wavefunctions of Gd^{3+} and Cm^{3+} are directly manifested in differences in the effects that a crystalline environment has on the ground-state splittings. In the case of the relatively pure $^8S_{7/2}$ Gd^{3+} ion in different crystalline hosts, splittings in the range of 0.1 to 1.0 cm^{-1} are found. The increased non-S-state character of the Cm^{3+} ion, on the other hand, leads to a relatively larger interaction with the crystal field and to the observation of ground-state splittings that are on the order of 10 to 50 cm^{-1}.

Other differences in the spectroscopic properties of the $4f^7$ and $5f^7$-configuration ions that are associated with corresponding differences in the non-S-state character of their ground-state wavefunctions are manifested in the observed EPR spin-lattice relaxation times. In the case of $4f^7$-configuration ions such as Gd^{3+}, the spin-lattice interaction times are relatively long, and the electron paramagnetic resonance absorption can be readily detected at room temperature. For the $5f^7$-configuration ions such as Cm^{3+}, however, the spin-lattice relaxation times are considerably shorter, and accordingly, cryogenic sample temperatures are generally necessary in order to observe the paramagnetic-resonance-absorption signals.

Historically, Cm^{3+} was the first $5f^7$-configuration ion observed by means of EPR spectroscopy. It should be pointed out, however, that the initial reports[1,2] of EPR spectra for Cm^{3+} ions in a $LaCl_3$ host (which resembled the spectra observed for Gd^{3+} in this same host) were quickly called into question based on the investigations of Marrus et al[3] and of Runciman.[4] Subsequent EPR investigations by Abraham et al.,[5] who grew Cm^{3+}-doped $LaCl_3$ single crystals with higher-purity starting material, showed that the actual Cm^{3+} EPR spectrum in $LaCl_3$ consisted of a single anisotropic line with values of $g_{||} = 1.925$ and $g_{\perp} = 7.67$. Accordingly, the initially reported results[1,2] were not due to Cm^{3+} but, in fact, represented the EPR spectrum of Gd^{3+}. EPR results were also obtained for Cm^{3+} in the trigonal host $La(C_2H_5SO_4)_3 \cdot 9H_2O$ in which a single anisotropic EPR transition with values of $g_{||} = 1.925(2)$ and $g_{\perp} = 7.73(2)$ was only observed at a temperature of 4 K. These observations provided additional confirmation of the interpretation of Abraham et al[5] regarding the earlier EPR results[1,2] which had been erroneously attributed to Cm^{3+} in the $LaCl_3$ host.

Following the initial observation of the actual EPR spectrum of Cm^{3+} in the $LaCl_3$ host (and in $La(C_2H_5SO_4)_3 \cdot 9H_2O$), the EPR spectra of Cm^{3+} and of the isoelectronic $5f^7$ ions Am^{2+} and Bk^{4+} have been reported[6–9] in a number of (predominantly cubic) host-crystal systems including CaF_2, SrF_2, BaF_2, $SrCl_2$, ThO_2 and CeO_2. For the specific case of Cm^{3+} in a cubic host, the cubic crystal field splits the eightfold-degenerate $J = 7/2$ ground manifold into three components—namely two doublets (Γ_6 and Γ_7) plus a Γ_8 quartet. Measurements of the anisotropic spectral features observed at high microwave frequencies for

Cm^{3+} in the cubic hosts have been used to determine the splittings between the ground Γ_6 doublet and the excited Γ_8 quartet. For comparison purposes, these results are summarized in Table 1 along with the comparable splittings for Gd^{3+} in the same hosts.[7]

When an f^7-electronic-configuration ion such as Cm^{3+} is subjected to a tetragonally symmetric crystal field, the degeneracy of the $^8S_{7/2}$ ground state will be removed by the formation of four doublet levels. For Cm^{3+} ions diluted in the tetragonally symmetric zircon-structure host $ThSiO_4$, however, no EPR spectra were observed[10]. This finding was accounted for based on the observation of a negative second-order spin-Hamiltonian parameter (b_2^0) for the $4f^7$ ion Gd^{3+} and the fact that the even larger negative parameter expected for Cm^{3+} would result in an isolated $|\pm 7/2\rangle$ ground-state doublet. In this case, no EPR transitions would be observed for such a doublet since the $g_\perp$ value would be zero.

The present work represents an extension of our previous investigation[11] of crystal-field-induced splittings of the ground state of Cm^{3+} in the tetragonal-symmetry host single crystal $LuPO_4$ where an excited-state EPR transition was observed. In this initial study of Cm in $LuPO_4$, a positive identification of the Cm^{3+} resonance was made by doping the $LuPO_4$ host with known relative concentrations of the two isotopes ^{243}Cm ($I = 5/2$) and ^{244}Cm ($I = 0$). The observed resonance was identified as arising from an excited-state doublet by observing that lowering the temperature reduced the intensity of the EPR signal. The experimentally determined axial g values of this doublet were fitted to a wavefunction of the form $\alpha|\pm 5/2\rangle + \beta|\mp 3/2\rangle$. In this case, the tetragonal symmetry of the crystal field produces $\Delta J_Z = \pm 4$ admixtures in the wavefunctions that result in non-zero $g_\perp$ values for each of the four doublets arising from the crystal-field splitting of the nominal $^8S_{7/2}$ ground state. Accordingly, transitions within each of the four doublets become allowed. The possibility of observing some of these additional allowed excited-state transitions led to a subsequent[12] combined EPR, optical, and Zeeman-effect study of curium in both $LuPO_4$ and YPO_4. The isotopes ^{243}Cm ($I = 5/2$) and ^{244}Cm ($I = 0$) were also used to identify the Cm^{3+} resonance in these investigations. In this case, EPR transitions were observed for three excited doublets in each orthophosphate host

crystal. For the YPO_4 host, the experimental axial g values were used to calculate the g values for the lowest-lying ground-state doublet (whose EPR was not observed). Optical-absorption and Zeeman-effect measurements yielded an experimental $g_{||}$ value for the lowest-lying doublet that was in excellent agreement with the value predicted on the basis of the EPR results.[12]

The present work reports the results of new EPR, optical absorption, and fluorescence measurements for Cm^{3+} in $LuPO_4$. Here the use of the isotope ^{248}Cm with its 3.4×10^5 year half life and lower specific activity (relative to the ^{244}Cm isotope present in the orthophosphate host crystals used in the two previous studies noted above[11,12]), reduced the broadening of the absorption lines induced by internal radiation damage. Through the use of these higher-quality samples, the EPR observation of an additional "inter-doublet" transition was possible. Additionally, new, more accurate measurements of the "intra-doublet" transitions were made using higher microwave frequencies (Q-band) rather than the X-band frequencies employed previously. The additional magnetic-resonance and optical data obtained here have led to a more accurate determination of the Cm^{3+} energy-level structure. Finally, the room-temperature Cm^{3+} magnetic-resonance spectrum reported here represents the first observation of an EPR transition at room temperature for an actinide ion.[13]

EXPERIMENTAL

The single crystals of $LuPO_4$ doped with $^{248}Cm^{3+}$ (or in some cases with $^{243,244}Cm$) and employed in this work were grown from a $Pb_2P_2O_7$ flux by means of a high-temperature solvent technique described previously.[14] In the case of the ^{248}Cm-doped specimens, the doping level corresponded to the addition of 10 mg of $^{248}CmO_2$ to 260 mg of Lu_2O_3. The doping level in the $^{243,244}Cm$-doped samples corresponded to the addition of 6 mg of $^{243,\ 244}CmO_2$ to 350 mg of Lu_2O_3. The ^{248}Cm-doped samples selected for the EPR and optical experiments were typically $5 \times 2 \times 1$ mm^3 with the long dimension of the crystal corresponding to the four-fold crystallographic c-axis. These specimens were transparent with a slight pink coloration. The crystals of $LuPO_4$ doped with $^{243,244}Cm$, however, turned black within a few days due to the radiation damage associated with the high specific activity of these isotopes. Annealing the

^{243,244}Cm-doped crystals at ~550°C for a few hours returned the material to its original state, although after several such annealings, the damage to the specimen appeared to be permanent, and the crystals remained a grey-to-black color that could not be removed by further annealing.

In carrying out the X-band (~9 GHz) EPR experiments, the Cm-doped crystals were mounted inside a Kel-F cylinder that was then inserted into a rectangular TE_{102}-mode microwave cavity so that the crystallographic c-axis lay in the horizontal plane. The EPR spectra could be recorded for sample temperatures ranging from ~2 to 350 K by using an Oxford Instruments model ESR-910 continuous flow cryostat. For the Q-band (~35 GHz) EPR experiments, the $LuPO_4$ single crystals were placed inside a segment of polyethylene tubing that was sealed at both ends and then inserted into the cylindrical TE_{011}-mode Q-band cavity. The Q-band EPR measurements could be performed with sample temperatures of 300 K, 77 K, and 4 K by using concentric double glass dewars.

The variation in the magnetic-field position of the anisotropic EPR transitions was determined by altering the angle between the crystal c-axis and the magnetic field direction by means of a rotating goniometer attached to the X-band microwave cavity. In the case of the Q-band EPR measurements, this angle could be varied directly by rotating the magnetic field. The microwaves were generated and the EPR signals detected using Varian E101 (X-Band) and E110 (Q-band) microwave bridges. Microwave-frequency measurements were made with an EIP-548 frequency counter, and the magnetic-field values were determined using a Varian E-500 NMR Gaussmeter.

RESULTS AND DISCUSSION

A. EPR Results

Examples of the X-band EPR spectra obtained at various sample temperatures for $^{248}Cm^{3+}$ in $LuPO_4$ are shown in Fig. 1. While a number of EPR lines were observed, by comparison with the known spectrum of Gd^{3+} in $LuPO_4$, it was possible to establish that only three of the transitions could actually be assigned to Cm^{3+} and that the remaining lines represented contributions from Gd^{3+}. This

assignment was further confirmed using the EPR spectrum of a $^{243,\ 244}Cm^{3+}$-doped $LuPO_4$ crystal where the distinct six-line hyperfine structure due to the I = 5/2, ^{243}Cm isotope (hyperfine coupling constant A = 23.14(4) G) could be resolved on the transitions that were due to trivalent curium. Additionally distinctions could be made between the characteristics of the Cm^{3+} and Gd^{3+} EPR lines. In general, the Gd^{3+} lines, which were narrower than the Cm^{3+} absorptions, could be easily saturated at low temperatures, and accordingly, these lines only interfered with the Cm^{3+} data collection when the magnetic-field orientation was such that the EPR transitions of the two elements overlapped.

The Cm^{3+} EPR transitions, which exhibited linewidths ranging from 20 to 80 Gauss, could be observed up to room temperature. The linewidths were, in fact, relatively independent of the sample temperature with the exception of the $|\pm 1/2\rangle$ transition whose linewidth narrowed significantly as the temperature was lowered. The observed intensity behavior of the EPR transitions with decreasing temperature indicates that the Cm^{3+} crystal-field states in the $LuPO_4$ host are relatively close in energy, i.e., large variations in the relative intensities of the transitions as a function of temperature were not observed. The observed resonance lines were assigned to the doublets: $|\pm 1/2\rangle$, $|\pm 3/2\rangle$, and $|\pm 5/2\rangle$, and the measured g-values were least-squares fit to the relation:

$$g^2 = g^2_{||} \cos^2\theta + g^2_{\perp} \sin^2\theta.$$

While the resonance of the $|\pm 7/2\rangle$ doublet could not be observed, its g-values were calculated using the admixture coefficients *a* and *b* obtained for the $|\pm 1/2\rangle$ doublet. The resulting g-values for all four doublets are given in Table 2 for the three sample temperatures 298 K, 77 K, and 4 K. In the case of the low-temperature g-values, the results were found to be in good agreement with those obtained in the earlier work.[12]

When the Cm^{3+}-doped $LuPO_4$ samples were examined using the higher Q-band frequency, additional EPR lines were observed; and up to six of these transitions could be attributed to Cm^{3+}. It was not possible, however, to determine the full angular variation for all of the observed Cm^{3+} transitions due either to rapid decreases in the absorption intensities as a function of the applied-field

orientation or to magnetic-field positions that exceeded the available maximum magnetic field. Other than the transitions that had already been observed in the X-band EPR experiments, it was possible to determine the angular variation for only one of the additional lines observed at Q-band. This transition occurred at a very low magnetic-field value and exhibited a large temperature dependence of its magnetic-field position (see Fig. 2). A similar transition was also observed for Cm^{3+} in the tetragonal YPO_4 host, but in this case, the temperature dependence was reversed. At room temperature with an applied magnetic field orientation $H_\perp$ c-axis ($\theta = 90°$), this resonance had a $g_\perp$ value of ~49 in $LuPO_4$ (or ~15 in YPO_4); but when the temperature was lowered to 77 K, the g-values shifted dramatically to $g_\perp$ ~22 for $LuPO_4$ (or $g_\perp$ ~18 for the YPO_4 host). This resonance cannot be assigned to a transition within any of the four Kramer's doublets and can only arise from a transition between different doublets. Such "inter-doublet" transitions are common in the case of $^8S_{7/2}$ lanthanide ions where the zero-field splittings are small, but they are somewhat unexpected in the case of the actinide ion Cm^{3+} since energy separations between two doublets (~35 GHz, 1.2 cm^{-1}) are required that are significantly smaller than any of the splittings determined previously (see Table 1). Additional experiments were performed in order to confirm the existence of this ~1 cm^{-1} splitting.

An additional anomaly was exhibited by this low-field resonance when the microwave frequency was changed. At room temperature and with the applied magnetic field oriented perpendicular to the crystallographic c-axis, the "intra-doublet" resonances for Cm^{3+} in $LuPO_4$ were all observed to shift to higher magnetic-field values as the microwave frequency was increased. In the case of the low-field resonance, however, the EPR line shifted to lower magnetic-field values with increasing microwave frequency (e.g., at a microwave frequency of 34.445 GHz the magnetic-field position of the line was 550 G while at 34.906 GHz, the line was located at 485 G).

It is possible to estimate the energy differences between the four ground-state doublets of Cm^{3+} by determining the temperature dependence of the intensities of the three "intra-doublet" resonances and by assuming that the positions of the crystal-field-level energies only undergo a slight variation with temperature. In carrying out this determination, Cm^{3+}:$LuPO_4$ spectra were recorded in the

temperature range from 10 K to 300 K. Careful measurements of the relative intensities of the observed transitions yielded a value of 5.8 ± 1.5 cm^{-1} for the energy difference between the $|\pm 5/2\rangle$ and $|\pm 3/2\rangle$ doublets and a value of 1.1 ± 0.5 cm^{-1} for the separation between the $|\pm 3/2\rangle$ and $|\pm 1/2\rangle$ doublets. Unless additional assumptions are made, the energy separation between the $|\pm 7/2\rangle$ and $|\pm 5/2\rangle$ doublets cannot be obtained. In any event, the results for the "inter-doublet" energies, coupled with the observed temperature dependence of the low-field transition, indicate that the low-field resonance is a transition between the $|\pm 3/2\rangle$ and $|\pm 1/2\rangle$ doublets. Since it is possible to make an assignment of this transition with some confidence based on the Q-band results, it was included along with the three "intra-doublet" resonance transitions in making a least-squares fit to the usual tetragonal spin-Hamiltonian—including both the Zeeman and crystal-field interactions.

The assignment of the "inter-doublet" transition effectively fixes the energy difference between the two doublets at a value of ~1.2 cm^{-1} and, therefore, significantly restricts the possibilities for choosing and varying the parameters. Among the four possibilities that exist for a transition between the $|\pm 3/2\rangle$ and $|\pm 1/2\rangle$ doublets, the best fit was obtained with the "inter-doublet" transition assigned as the transition between the upper Zeeman level of the $|\pm 3/2\rangle$ doublet and the lower Zeeman level of the $|\pm 1/2\rangle$ doublet. The spin-Hamiltonian parameters corresponding to the best fit are given in Table 3 along with the calculated zero-field energies. A calculated fit to the experimental data is illustrated in Fig. 3. In the case of the three other possible assignments, the fits were not as good even though convergence could be obtained. Nevertheless, the parameters obtained from the other fits agreed to within 20% with the "best-fit" parameters, and the calculated zero-field energies are within ±2 cm^{-1} when compared with the "best fit" values.

The calculated zero-field energy differences at 10 K are 1.4 cm^{-1} and 6.2 cm^{-1} for the $|\pm 3/2\rangle \rightarrow |\pm 1/2\rangle$, and $|\pm 5/2\rangle \rightarrow |\pm 3/2\rangle$ separations respectively, and these values are in good agreement with the results obtained from the temperature-dependence investigation. For the case of the $|\pm 7/2\rangle \rightarrow |\pm 5/2\rangle$ separation, the calculated energy difference is 3.8 cm^{-1}. In Fig. 4 , the calculated energy levels of the four ground doublets of Cm^{3+} in $LuPO_4$ are plotted as a function of the applied magnetic field for a sample temperature of

77 K with the applied magetic field oriented perpendicular to the c- crystal axis. The observed relatively large temperature dependence exhibited by the "inter-doublet" transition can now be understood by referring to Fig. 4. The calculated energy separation between the $|\pm 3/2\rangle$ and $|\pm 1/2\rangle$ doublets is 1.4 cm^{-1} and 1.3 cm^{-1} at 10 K and 298 K, respectively. The difference of 0.1 cm^{-1} for the different sample temperatures is significant in the microwave frequency range, and consequently, a relatively large shift in the resonance field with temperature will occur. Additionally, from Fig. 4 it can be seen that an increase in the Q-band frequency will shift this resonance to lower magnetic field.

In the case of Cm^{3+} in the cubic fluorite-structure host $SrCl_2$ (the only other system where the complete Cm^{3+} zero-field splitting has been determined), the Cm^{3+} EPR signals can be detected at temperatures as high as 200 K.[9] For the Cm^{3+}:$SrCl_2$ system, the zero-field splitting is 20.43 cm^{-1}. The zero-field splitting for Cm^{3+} in the tetragonal symmetry site of $LuPO_4$ is about one-half that of the splitting for Cm^{3+} in $SrCl_2$. It is, therefore, reasonable that the Cm^{3+} EPR transition can be observed at room temperature for the $LuPO_4$ host. On this same basis, however, it is somewhat surprising that Cm^{3+} EPR signals have not been observed above 4 K for the hexagonal-symmetry host $LaCl_3$[5,11]

B. Optical Results

The amount and type of information that can be obtained by means of EPR spectroscopy is effectively limited by its restricted energy range and the number and type of transitions that can be detected and assigned. Optical spectroscopy, on the other hand can generally be used to obtain information over a much wider energy range, and accordingly, optical methods were used to support and confirm the EPR results for Cm^{3+} in $LuPO_4$. In fact, in the present case of Cm^{3+} in $LuPO_4$, the total zero-field splitting of the ground state of ~10 cm^{-1} and the energy separations between the four Kramer's doublets of 1 to 7 cm^{-1} can be readily resolved by means of optical spectroscopy where a resolution of 0.1 to 1.0 cm^{-1} can be achieved. Additionally, optical spectroscopy provides information on the crystal-field splittings of the excited electronic states and on the energy separation between the crystal-field-split manifolds.

In D_{2d} symmetry, all half-integral J manifolds of the f^7 configuration decompose into (2J+1)/2 Kramers' doublets with labels of Γ_6 or Γ_7. The selection rules are the same for both absorption and emission spectroscopies, and the allowed electric-dipole transitions are:

$$\sigma\begin{cases}\Gamma_6 \rightarrow \Gamma_6, \Gamma_7 \\ \Gamma_7 \rightarrow \Gamma_6, \Gamma_7\end{cases}$$

$$\pi\left\{\Gamma_7 \leftrightarrow \Gamma_6\right.$$

where π is the polarization of the electric field along the z direction (crystal c-axis $\vec{E} \mid \mid c$), and σ is the polarization of the electric field along the x (or y) direction ($\vec{E} \perp c$). From the EPR results, the total zero-field splitting of the ground J = 7/2 state was found to be ~10 cm^{-1}. Therefore a population of and absorption from every doublet of the ground manifold is expected.

In general, the measured optical-absorption spectra at 4 K for Cm^{3+} in $LuPO_4$ showed relatively sharp (FWHM of 1-2 cm^{-1}), but very weak lines. This weak intensity limited the accuracy of the optical measurement. Fewer lines than were theoretically predicted could be detected. Below 24,000 cm^{-1}, only nine out of eighteen predicted transitions were observed, and only four lines were detected above 24,000 cm^{-1}. This weak intensity is, in part, due to the low concentration of Cm^{3+} present in the crystals. The absorption lines did not exhibit very well defined polarization characteristics which made their assignments difficult. Accordingly, a consistent set of crystal-field parameters could not be obtained. In addition, the total splittings of the excited-state J = 7/2 manifolds could not be determined since only two crystal-field states were found in each of the $^6D_{7/2}$ and $^6I_{7/2}$ free-ion states. The cummulative results for the measured energy levels of the Cm^{3+}:$LuPO_4$ system are summarized in Table 4.

Many of the observed transitions occurred in groups of two or three, spread over a region of <10 cm^{-1}, instead of appearing as a single line, and this fine structure undoubtedly arises from the ground manifold of Cm^{3+}. (Splittings of excited states by the crystal field are normally on the order of tens to hundreds of

wavenumbers.) Using the knowledge of the zero-field splitting as determined from the EPR data, it is straightforward to interpret these lines. Of the thirteen transitions recorded, all but three of the weakest exhibited fine structure. Most of these showed a splitting of 3.2–3.8 cm^{-1}, and for some, a second splitting of 7.4–10.0 cm^{-1} was also observed. However, none of the transitions showed the quartet structure as expected. The inability to observe a fourth line in the fine structure is probably due to a combination of i) a low population of the highest state of the ground manifold, ii) a low probability for transitions arising from this state, and iii) the broadness of the peak widths which cannot be resolved. Both the polarized and unpolarized spectra recorded at 77 K are relatively similar, and the room-temperature spectra exhibit significantly broader peak widths with much of the fine structure unresolved. Hence, although the optical absorption data for the splittings are consistent with the EPR data, in fact, information that was more precise than the EPR results was not obtained by this technique.

Excitation spectroscopy is inherently more sensitive than absorption spectroscopy in probing the line positions of excited states. Therefore, a tunable dye laser (Coumarin 487) pumped by an argon laser was used to provide excitation in the range from 19,500 to 21,000 cm^{-1}. The $^{248}Cm:LuPO_4$ specimen was maintained at a temperature of ~10 K during the excitation measurements, and the fluorescence intensity of the 16,528 cm^{-1} line was monitored while the excitation frequency was scanned. The resulting spectrum is shown in Fig. 5. Three relatively sharp lines plus a very weak shoulder were observed. These three lines are also observed in the 77 K absorption spectrum at $\approx$ 19,770 cm^{-1}, which is also included in Fig. 5 for comparison. The shoulder, which was not observed in the less-sensitive absorption spectrum, is assigned to the absorption originating from the highest doublet of the ground manifold. Its low intensity is probably due to a very small transition probability rather than the low population since the absorption arising from the next-highest doublet (which is only 1.4 cm^{-1} away) is much stronger. The splittings of the ground manifold are determined to be 0.0, 3.6, 8.5 and 9.9 cm^{-1}. These values are to be compared with the values of 0.0, 3.8, 10.0 and 11.4 cm^{-1} as measured by EPR spectroscopy at 4 K.

A second peak was found at an excitation frequency of 20,180 cm^{-1}. This peak is very weak and broad, but it appears to have the same overall width ($\approx$ 10 cm^{-1}) and profile as the group at 19,775 cm^{-1}. Since this peak does not correspond to

any line in the absorption spectrum (see Table 4) or exhibit any fine structure, it was not investigated further.

The fluorescence spectra of Cm^{3+} in $LuPO_4$ were obtained with an argon-ion laser providing the excitation. The emission photons were collected at an angle of 90° relative to the laser-excitation photons and were analyzed using a SPEX 1403 double monochromator. The results are tabulated and summarized in Table 5. These results are reminiscent of the absorption peaks—i.e., they are relatively quite weak and do not exhibit well-defined polarization characteristics. With the exception of the peak at 16,575.4 cm^{-1}, they all show splittings of 3.2-3.5 cm^{-1} and 8.1–8.8 cm^{-1}, but again no quartet structure is apparent. Consequently, in a manner similar to the absorption spectra, they are consistent with the EPR results.

DISCUSSION

In fitting the experimental data obtained for Cm^{3+} in $LaCl_3$, Carnall[17] noted that employing the crystal-field parameters determined for Bk^{3+} in $LaCl_3$ resulted in a better fit (lower error) to the observed levels of Cm^{3+}:$LaCl_3$, than did the set obtained for Am^{3+}in $LaCl_3$. When allowed to vary freely, the crystal-field parameters for Cm^{3+}in $LaCl_3$ took on values somewhat intermediate between those of Am^{3+} and Bk^{3+}. The fit did not, however, result in a lower error than that obtained with the crystal-field parameters derived for Bk^{3+} in $LaCl_3$. Both the EPR data[5] and the fluorescence results[18] for Cm^{3+} in $LaCl_3$ were interpreted as identifying the ground state as $J_z = |\pm 1/2\rangle$ which is inconsistent with the computed ordering of the ground-state levels. Carnall[17] concluded that the total splitting was <8 cm^{-1} and that the ground state was $J_z = |\pm 7/2\rangle$ and "considered the discrepancy to represent an unresolved problem." While the calculated splitting cannot be given too much significance due to the large uncertainties associated with the determined parameters and the large number of levels to be fit over an extended range (>30,000 cm^{-1}), it raises the question: How well can the zero-field splitting of the ground S-state of Cm^{3+} be described by the crystal-field splitting of the excited states through intermediate coupling? Recently, the zero-field splitting of a Gd^{3+} S-state was found to be a reflection of the crystal-field splitting of the excited $^6P_{7/2}$ manifold.[19] It is expected that crystal-field

parameters of the excited states are more applicable to Cm^{3+} S-state splittings than to Gd^{3+} S-state splittings since intermediate-coupling effects are significantly larger for the actinide ion. The calculated ground S-state levels in Cm^{3+}:$LuPO_4$ using the free-ion parameters of Cm^{3+} in $LaCl_3$ and crystal-field parameters for Nd:YPO_4 lie at 2.3, 7.3 and 7.7 cm^{-1}.

No crystal-field parameter for any actinide in $LuPO_4$ is currently available, and the splittings of the $^6D_{7/2}$ or the $^6I_{7/2}$ manifolds in Cm^{3+}:$LuPO_4$ could not be determined. If the large intermediate-coupling effect is the most important zero-field-splitting mechanism in Cm^{3+}:$LuPO_4$, then the spin-Hamiltonian parameters can be related to the crystal-field parameters through the use of operator-equivalent factors.[20] The resulting crystal-field parameters can then be used to calculate the wavefunctions of the crystal-field states of the neighboring actinides in $LuPO_4$. Such an approach relies on the expectation that crystal-field parameters of neighboring elements do not show large variations—an assumption that is often borne out by experiment. For example, the ground crystal-field state of Np^{4+} in $ZrSiO_4$ (D_{2d} site symmetry) was calculated to be a Γ_6 doublet by using the free-ion parameters of Np^{4+}:$Zr(BD_4)_4$ and the crystal-field parameters of U^{4+}:$ZrSiO_4$. This result was experimentally confirmed by EPR.[21] The ion Pu^{4+} in $ZrSiO_4$ was also found to have very similar crystal-field parameters.[22] For the present purposes, the g-values of the electronic ground states in Pu^{3+}:$LuPO_4$ and Cf^{3+}:$LuPO_4$ have been determined by EPR[23] and compared to those calculated by using free-ion parameters from crystal-field analyses of Pu^{3+}, Cf^{3+}:$LaCl_3$[17] plus a set of crystal-field parameters obtained from the Cm^{3+} spin-Hamiltonian parameters using the operator equivalent factor method. Operator equivalent factors have been calculated for a 50-term Cm^{3+} wavefunction,[24] and they are used here, together with tabulated conversion factors,[25] to obtain the following "crystal-field parameters" following the Wybourne convention[26] for Cm^{3+}:$LuPO_4$ (in cm^{-1} at 10K): $B_0^2 = 446$, $B_0^4 = 322$, $B_0^6 = -850$, $B_4^4 = -1{,}080$, and $B_4^6 = 818$.

SUMMARY

The zero-field splitting of Cm^{3+} incorporated into $LuPO_4$ has been determined by EPR, and the results obtained from additional optical fluorescence and

absorption experiments are found to be in reasonable agreement with those obtained from the X- and Q-band resonance measurements. Although the splitting is large compared to the microwave frequencies employed, four transitions could be assigned and were fit to give a consistent set of spin-Hamiltonian parameters. The total splitting of ≈ 10 cm^{-1} is considerably smaller than the only previously known Cm^{3+} zero-field splitting of 20.4 cm^{-1} determined for the cubic host $SrCl_2$. The somewhat unexpectedly small crystal field is probably responsible for the first observation of room-temperature EPR of an actinide ion. The cause of this significant decrease in the total zero-field splitting of Cm^{3+} is not accounted for. It is unfortunate that the crystal-field data for the excited states are not presently available so that a more detailed comparison could be made between the splittings of the ground and excited manifolds in order to shed additional light on the mechanisms that affect these splittings.

Acknowledgement

This research was sponsored by the Division of Materials Sciences, U.S. Department of Energy under Contract No. DE-AC05-84OR21400 with Martin Marietta Energy Systems, Inc., and by the Director, Office of Energy Research, Office of Basic Energy Sciences, Chemical Sciences Division of the U.S. Department of Energy under Contract No. DE-AC03-76SF00098. The authors are indebted, for the use of ^{248}Cm, to the Division of Chemical Sciences, Office of Basic Energy Sciences, through the transplutonium element production facilities at Oak Ridge National Laboratory. The authors also acknowledge with thanks the excellent technical contributions of H.E. Harmon and C.B. Finch.

References

1. M. M. Abraham, B. B. Cunningham, C. D. Jeffries, R. W. Kedzie, and J. C. Wallmann, *Bull. Am. Phys. Soc.* **1**, 396 (1956).
2. P. Fields, A. Friedman, B. Smaller, and W. Low, *Phys. Rev.* **105**, 757 (1957).
3. R. Marrus, W. A. Nierenberg, and J. Winocur, *Phys. Rev.* **120**, 1429 (1960)
4. W. A. Runciman, *J. Chem. Phys.* **36**, 1481 (1962).
5. M. M. Abraham, B. R. Judd, and H. H. Wickman, *Phys. Rev.* **130**, 611 (1963).
6. N. Edelstein, in *Americium and Curium Chemistry and Technology*, ed. by N. M. Edelstein, J. D. Navratil, and W. W. Schulz, D. Reidel Publishing Co. Dordrecht/Boston/Lancaster, 1985, p. 193.
7. W. Kolbe, N. Edelstein, C. B. Finch, and M. M. Abraham, *J. Chem. Phys.* **58**, 820 (1973), [*Erratum*, ibid, **59**, 1568 (1973)].
8. W. Kolbe, N. Edelstein, C. B. Finch, and M. M. Abraham, *J. Chem. Phys.* **56**, 5432 (1972).
9. M. M. Abraham, L.A. Boatner, C.B. Finch, R.W. Reynolds, and H. Zeldes, *Phys. Rev. B* **1**, 3555 (1970).
10. M. M. Abraham, G. W. Clark, C. B. Finch, R. W. Reynolds, and H. Zeldes, *J. Chem. Phys.* **50**, 2057 (1969).
11. M. M. Abraham and L. A. Boatner, *Phys. Rev. B* **26**, 1434 (1982).
12. M. M. Abraham, L. A. Boatner, C. B. Finch, W. K. Kot, J. G. Conway, G. V. Shalimoff, and N. M. Edelstein, *Phys. Rev. B* **35**, 3057 (1987).
13. L. A. Boatner and M. M. Abraham, *Repts. Prog. Phys.* **41**, 87 (1978).
14. M. M. Abraham, L. A. Boatner, and J. O. Ramey, *J. Chem. Phys.* **83**, 2754 (1985).

15. M. Rappaz, L. A. Boatner, and M. M. Abraham, *J. Chem. Phys.* **73**, 1095 (1980).

16. M. M. Abraham, L. A. Boatner, C. B. Finch, R. W. Reynolds, and W. P. Unruh, *Phys. Lett.* **44A**, 527 (1973).

17. W. T. Carnall, Argonne National Laboratory, ANL-89/39 (1989).

18. J. B. Gruber, W.R. Cochran, J.G. Conway, and A.T. Nicol, *J. Chem. Phys.* **45**, 1423 (1966).

19. S.K. Misra and N.R. Lewis, *Phys. Rev. B* **31**, 8335 (1985).

20. See A. Abragam and B. Bleaney, *Electron Paramagnetic Resonance of Transition Ions*, (Oxford University Press, London 1970).

21. I. Poirot, W. Kot, N. Edelstein, M.M. Abraham, C.B. Finch, and L.A. Boatner, *Phys. Rev. B* **37**, 3255 (1988).

22. I.S. Poirot, W.K. Kot, N. Edelstein, M.M. Abraham, C.B. Finch, and L.A. Boatner, *Phys. Rev. B* **39**, 6388 (1989).

23. W.K. Kot, N.M. Edelstein, M.M. Abraham, and L.A. Boatner (to be published).

24. N. Edelstein and W. Easley, *J. Chem. Phys.* **48**, 2110 (1968).

25. J. Kassman, *J. Chem. Phys.* **52**, 2117 (1970).

26. B.G. Wybourne, *Spectroscopic Properties of Rare Earths*, (Wiley, New York 1965) p. 164.

Table 1. $\Gamma_8 \rightarrow \Gamma_6$ Splitting of the Trivalent $4f^7$ and $5f^7$ *S*-State Ions in Cubic Crystal Fields at 4.2°K (after Kolbe et al., (1973)).

Host	Lattice Constant (Å)	Gd^{3+} (cm^{-1})	Cm^{3+} (cm^{-1})
CeO_2	5.41	0.0653 ± 0.0004	17.8 ± 0.3
ThO_2	5.60	0.06645 ± 0.00008	15.5 ± 0.3
CaF_2	5.46	0.0578 ± 0.0001	13.4 ± 0.5
SrF_2	5.80	0.0501 ± 0.0002	11.2 ± 0.4
BaF_2	6.20	0.0448 ± 0.0002	---
$SrCl_2$	7.00	0.01979 ± 0.00004	5.13 ± 0.05

Table 2. Measured g-values of Cm^{3+}:$LuPO_4$ at Various Temperatures (Microwave Frequency = 9.17 to 9.32 GHz). [a]Calculated using $g_J = 1.925$.

Temperature	298 K		77 K		4 K	
	$g_{\|\|}$	$g_\perp$	$g_{\|\|}$	$g_\perp$	$g_{\|\|}$	$g_\perp$
$a \mid \pm 1/2\rangle + b \mid \mp 7/2\rangle$	1.46(3)	7.34(10)	1.422(3)	7.341(10)	1.380(3)	7.284(10)
$c \mid \pm 3/2\rangle + d \mid \mp 5/2\rangle$	4.17(2)	3.98(2)	4.15(1)	4.08(2)	4.12(1)	4.10(1)
$c \mid \pm 5/2\rangle - d \mid \mp 3/2\rangle$	8.06(4)	3.98(2)	7.971(5)	4.08(2)	7.977(5)	4.102(2)
$a \mid \pm 7/2\rangle - b \mid \mp 1/2\rangle$	(12.79)[a]	(0.21)[a]	(12.72)[a]	(0.23)[a]	(12.69)[a]	(0.25)[a]

Table 3. Spin-Hamiltonian Parameters and Calculated Zero-Field Energies of Cm^{3+}:$LuPO_4$ at Various Temperatures. See Refs. 11 and 12 for the definition of the b_k^q parameters.

Temperature	298 K	77 K	10 K
g_J	1.925	1.925	1.925
b_2^0 (cm^{-1})	-0.741	-0.910	-0.936
b_4^0 (cm^{-1})	0.074	0.056	0.051
b_6^0 (cm^{-1})	0.056	0.059	0.060
b_4^4 (cm^{-1})	-1.036	-1.347	-1.429
b_6^4 (cm^{-1})	-0.146	-0.608	-0.645

Table 4. Absorption Spectrum of Cm^{3+}:$LuPO_4$ at 4.2°K

SLJ State	Experimental (cm^{-1})			
	σ-spectrum		π-spectrum	
$^8S_{7/2}$				
$^6D_{7/2}$	16528.3 cm^{-1}		16528.3 cm^{-1}	
	16524.9	Δ = 3.4		
	16519.9	Δ = 8.4	16519.9	Δ = 8.4
	16577.5		16577.3	
	---		---	
	---		---	
$^6D_{5/2}$	19775.3		19775.4	
	19771.8	Δ = 3.5		
	19767.9	Δ = 7.4	19767.5	Δ = 7.9
	---		---	
	---		---	
$^6I_{7/2}$	---		---	
	---		---	
			21445.3	
	21441.6	Δ = 3.7		
	21437.7	Δ = 7.6	21437.1	Δ = 8.2
	21471.7			
			21468.6	Δ = 3.1
	21463.6	Δ = 8.1		

Table 4. (continued)

SLJ State	Experimental (cm^{-1})			
	σ-Spectrum		π-Spectrum	
$^6P_{3/2}$	22034.1		22034.1	
	22137.1		22137.0	
$^6I_{9/2}$	—		—	
	—		—	
	22585.0		—	
	22581.2	Δ = 3.8		
	22575.9	Δ = 9.1	22575.0	Δ = 10.0
	22664.5		22664.8	
	22661.3	Δ = 3.2		
	19767.9	Δ = 7.4	19767.5	Δ = 7.9
$^6I_{17/2}$	24612.3			
$^6I_{11/2}$	24608.9	Δ = 3.4	24608.7	Δ = 3.4
	24603.3	Δ = 9.0		
	24690.8		24690.8	
	24687.0	Δ = 3.2		
	24682.8	Δ = 8.0	24682.0	Δ = 8.8
	24792.5		24792.7	
	24784.0	Δ = 8.5		

Table 5. Fluorescence spectra of Cm^{3+}:$LuPO_4$ at 10 K excited with the argon ion line at 496 nm (20,156 cm^{-1}).

σ-Polarization		π-Polarization	
16528.4 cm^{-1}(s)		16528.4 cm^{-1}(s)	
16525.0 (w)	Δ = 3.4 cm^{-1}	16525.0 9 (w)	Δ = 3.4 cm-1
16519.6 (s)	Δ = 8.8	16519.6 (m)	Δ = 8.8
16575.4 (br)			
19775.7cm^{-1}(w)		19775.4 cm^{-1}(s)	
19772.2 (w)	Δ = 3.5 cm^{-1}	19772.2 (w)	Δ = 3.2 cm^{-1}
19767.5 (s)	Δ = 8.2	19767.3 (m)	Δ = 8.1

Figure Captions

Fig. 1. EPR spectra of Cm^{3+}:$LuPO_4$ at various temperatures (peaks not labelled are due to Gd^{3+} impurities) Microwave Frequency = 9.235 GHz and $\theta = 0°$. (H || C)

Fig. 2. Angular and temperature dependence of the Q-Band EPR low-field transitions in Cm^{3+}:$LuPO_4$ (open symbols) and Cm^{3+}:YPO_4 (solid symbols). Microwave Frequency = 34.885 GHz. 0° is H || C.

Fig. 3. Experimental and fitted dependence of the EPR spectra as a function of the angle between the crystallographic *c* axis and the magnetic field. (A) Microwave frequency = 9.235 GHz, 77 K and (B) Microwave frequency = 9.4 and 34.742 GHz, room temperature.

Fig.4. Calculated Zeeman energy levels for Cm^{3+}:$LuPO_4$ and the observed X (0.3 cm^{-1}) and Q (1.2 cm^{-1}) band EPR transitions with the magnetic field perpendicular to the crystallographic *c* axis at 77 K.

Fig.5. The excitation spectrum of Cm^{3+}:$LuPO_4$ at 10 K and the absorption spectrum at 77 K. The x-axis is the excitation and absorption frequency; the fluorescence intensity was measured at 16,528 cm^{-1}. No polarization was used and the measured peakwidths of the excitation spectrum (FWHM) are, from left to right, 1.5 cm^{-1}, 1.2 cm^{-1}, and 1.2 cm^{-1}.

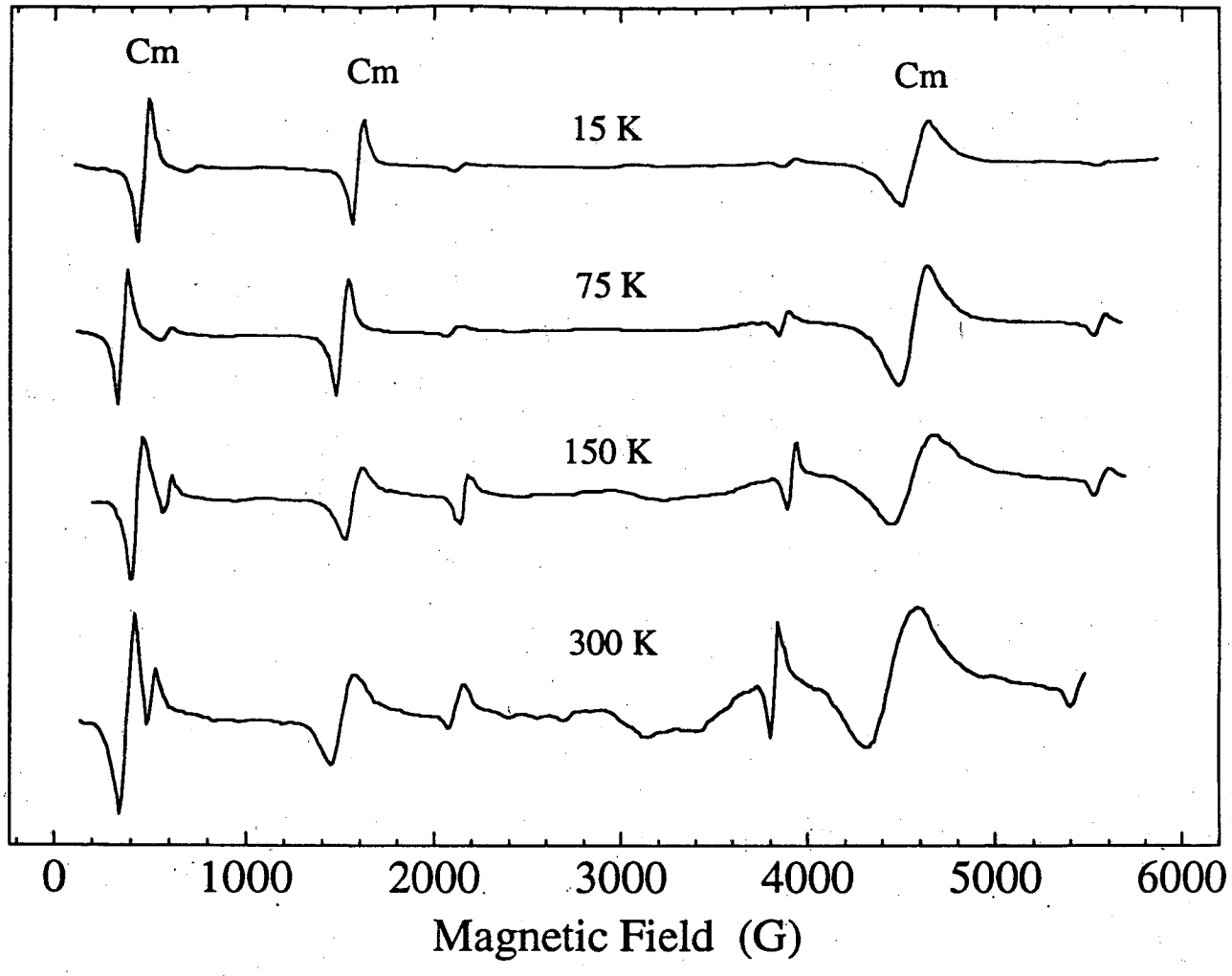
Cm
Cm
Cm
15 K
75 K
150 K
300 K
0
1000
2000
3000
4000
5000
6000
Magnetic Field (G)

Figure 1

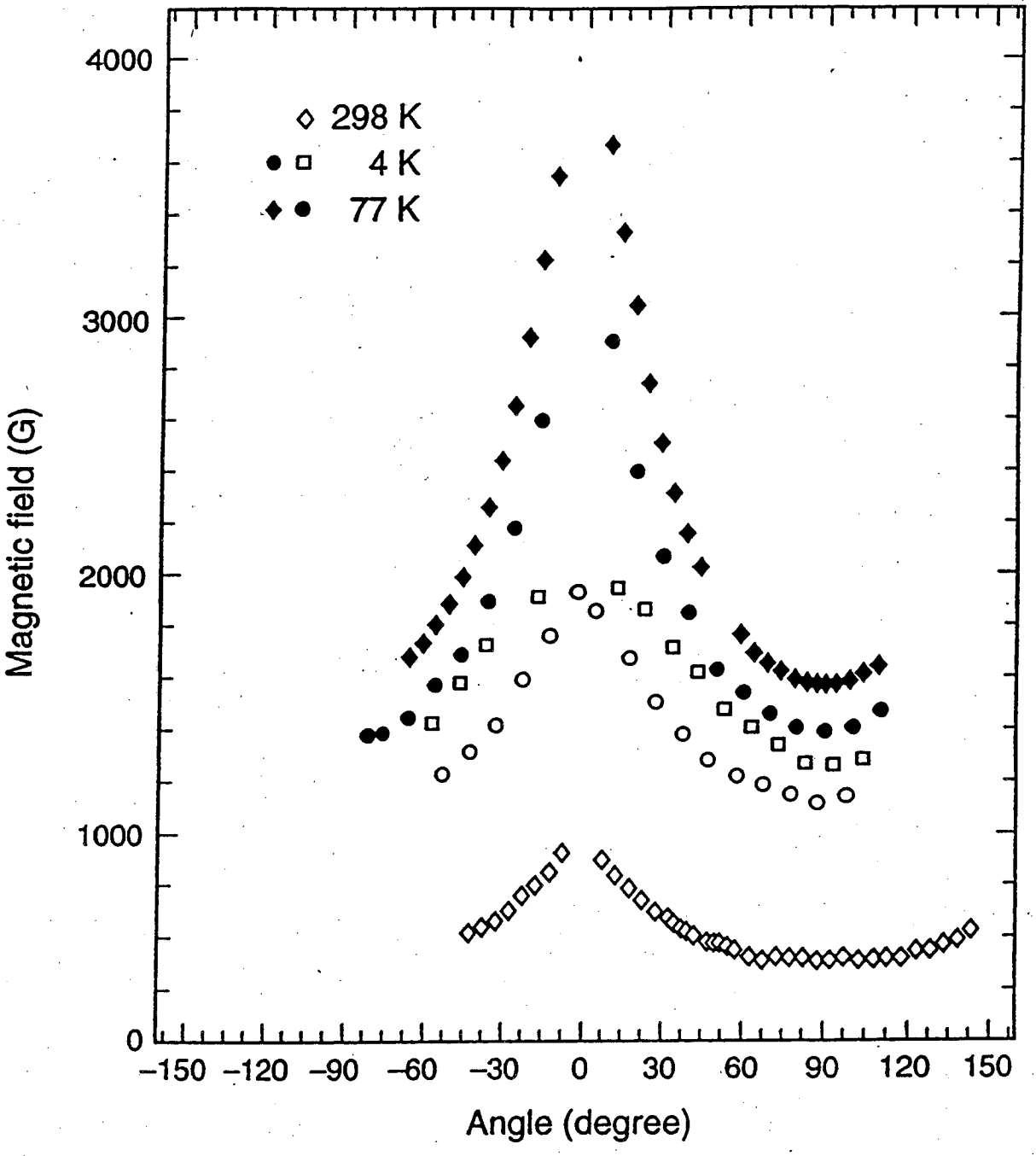
298 K
4 K
77 K
Magnetic field (G)
4000
3000
2000
1000
0
−150 −120 −90 −60 −30 0 30 60 90 120 150
Angle (degree)
XBL 927-5733

Figure 2

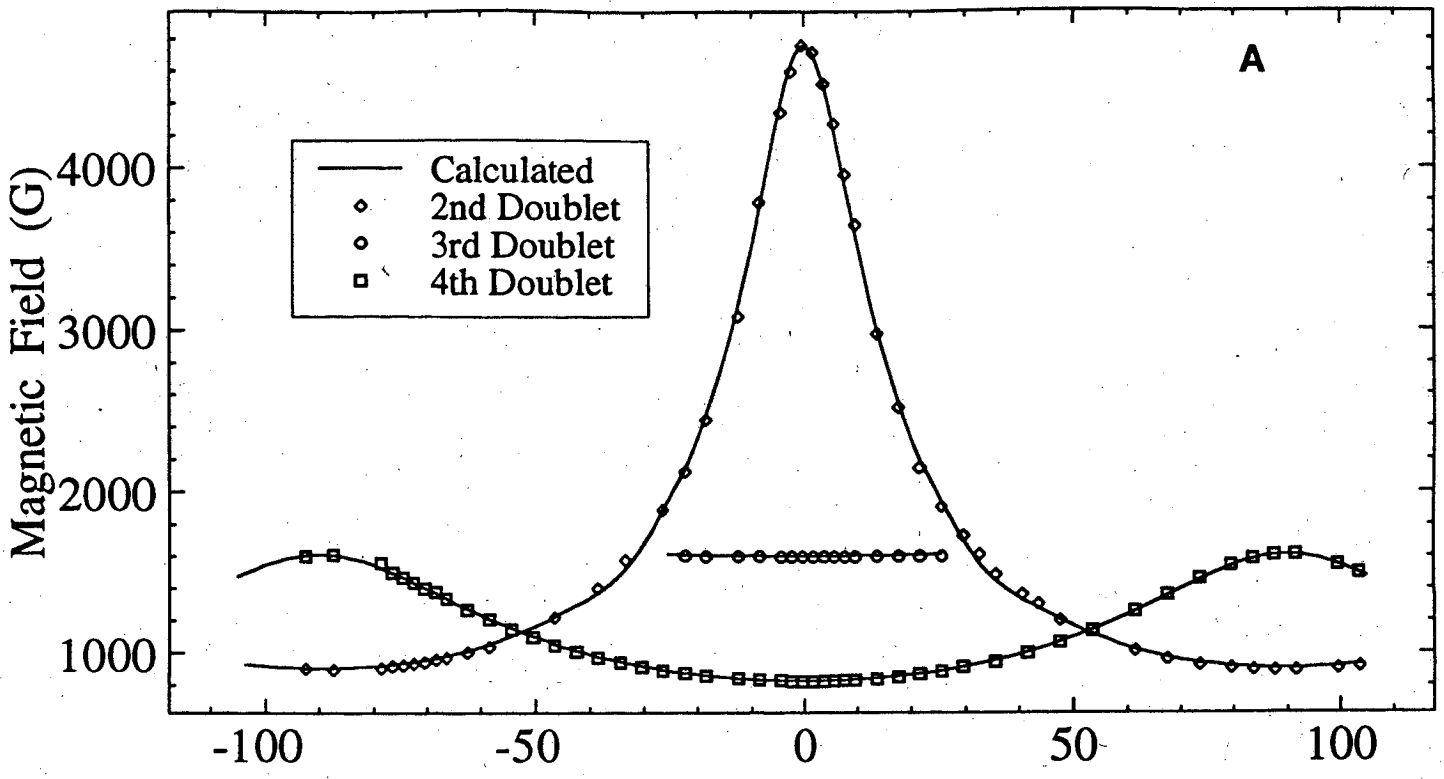
A
Calculated
2nd Doublet
3rd Doublet
4th Doublet
Magnetic Field (G)
4000
3000
2000
1000
-100
-50
0
50
100

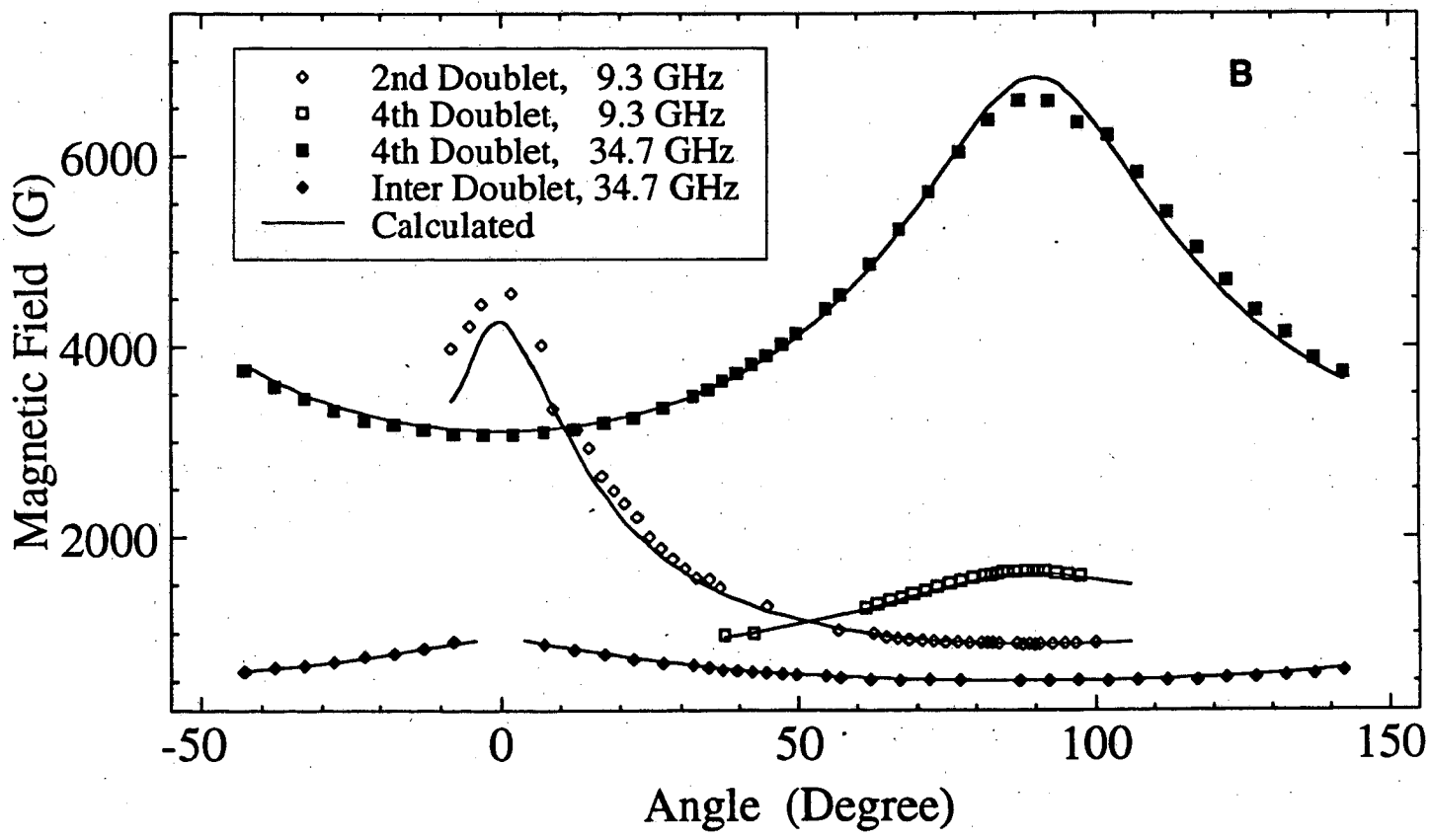
B
2nd Doublet, 9.3 GHz
4th Doublet, 9.3 GHz
4th Doublet, 34.7 GHz
Inter Doublet, 34.7 GHz
Calculated
Magnetic Field (G)
6000
4000
2000
-50
0
50
100
150
Angle (Degree)

Figure 3

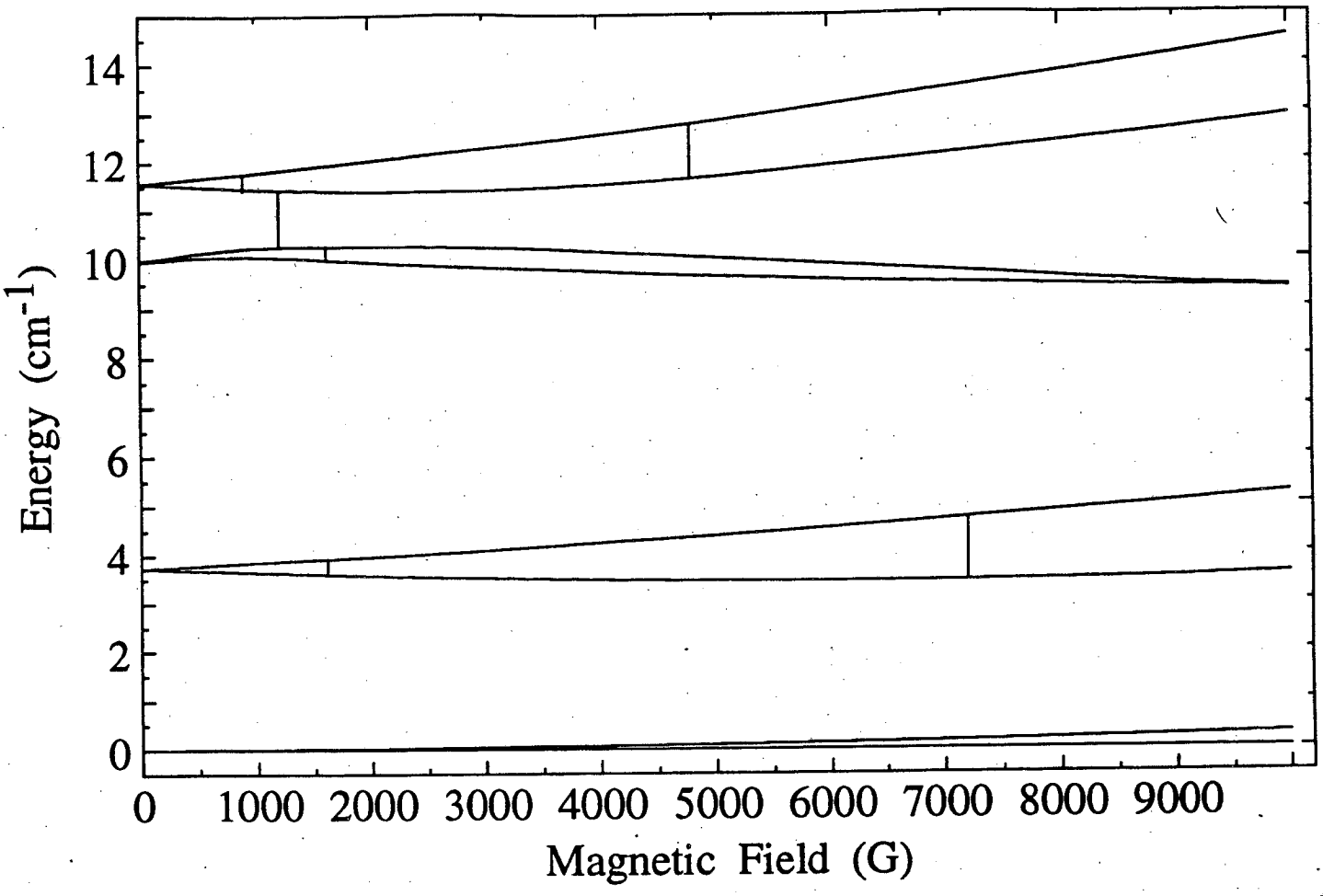
Energy (cm-1)
14
12
10
8
6
4
2
0
0
1000
2000
3000
4000
5000
6000
7000
8000
9000
Magnetic Field (G)

Figure 4

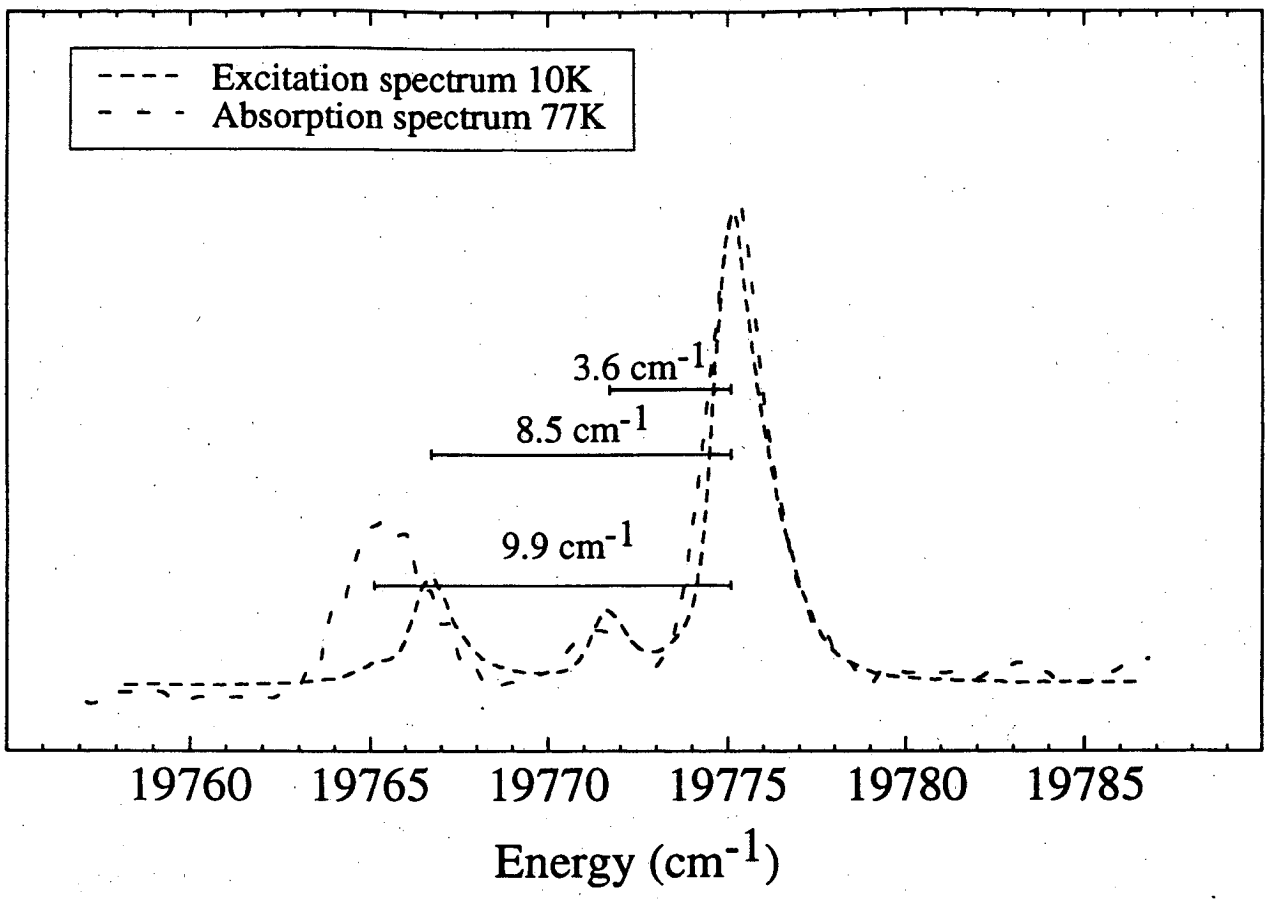
Excitation spectrum 10K
Absorption spectrum 77K
3.6 cm-1
8.5 cm-1
9.9 cm-1
19760
19765
19770
19775
19780
19785
Energy (cm-1)

Figure 5

LAWRENCE BERKELEY LABORATORY
UNIVERSITY OF CALIFORNIA
TECHNICAL INFORMATION DEPARTMENT
BERKELEY, CALIFORNIA 94720